DOI: 10.1002/cbic.201100714

Directed Evolution of Subtilisin E into a Highly Active and Guanidinium Chloride- and Sodium Dodecylsulfate-Tolerant Protease

Zhenwei Li,[a, b] Danilo Roccatano,[b] Michael Lorenz,[c] and Ulrich Schwaneberg*[a]

Proteases have niche applications in diagnostic kits that use cell lysis and thereby require high resistance towards chaotropic salts and detergents, such as guanidinium chloride (GdmCl) and sodium dodecylsulfate (SDS). Subtilisin E, a well-studied serine protease, was selected to be re-engineered by directed evolution into a "chaophilic" protease that would be resistance to GdmCl and SDS, for application in diagnostic kits. In three iterative rounds of directed evolution, variant SeSaM1–5 (S62I/A153V/G166S/I205V) was generated, with improved activity (330%) and increased half life in 1 M GdmCl (< 2 min to 4.7 h) or in 0.5% SDS (< 2 min to 2.7 h). Saturation mutagenesis at each site in the wild-type subtilisin E revealed that positions 62 and 166 were mainly responsible for increased activity and stability. A double mutant, M2 (S62I/G166M), generated by combination of the best single mutations showed significantly improved kinetic constants; in 2 M GdmCl the K_m value decreased (29-fold) from 7.31 to 0.25 mM, and the k_{cat} values increased (fourfold) from 15 to 61 s^{-1}. The catalytic efficiency, k_{cat}/K_m, improved dramatically (GdmCl: 247 $mM^{-1}s^{-1}$ (118-fold); SDS, 179 $mM^{-1}s^{-1}$ (13-fold)). In addition, the SeSaM1–5 variant showed higher stability in 2.0% SDS when compared to the wild-type ($t_{1/2}$ 54.8 min (> 27-fold)). Finally, molecular dynamics simulations of the wild-type subtilisin E showed that Gdm^+ ions could directly interact with active site residues, thereby probably limiting access of the substrate to the catalytic centre.

Introduction

Proteases have a broad range of industrial applications, in detergents, food, pharmaceuticals, leather treatment, diagnostics, waste management, and silver recovery.[1] Attractive niche markets are DNA-sequence-based diagnostic kits to rapidly diagnose diseases or pathogens from enriched DNA samples. Cell lysis and efficient DNA extraction requires proteases that are stable in chaotropic salts, such as guanidinium chloride (GdmCl), guanidine thiocyanate (GdmSCN), and/or detergents (SDS or Tweens).[2]

Chaophiles (chaophilic microbes) represent a new class of extremophilic microbes that prefer chaotropic conditions.[3] The terms "chaophilic" or "chaotolerant" refer to proteases that prefer or tolerate chaotropic conditions. Halophilic and thermophilic proteases are the natural first choice for applications with chaotropic conditions. Halophilic proteases have been mainly reported from Archaea,[4] and less frequently from bacteria.[5] Halophilic proteases often preserve high activity, solubility, and stability in the presence of high salt concentrations ($\leq$ 4 M); however, they are often denaturated by GdmCl at concentrations above 3 M.[6] Of hyperthermophilic proteases, the recently discovered Tk-subtilisin from *Thermococcus kodakaraensis* seems to be most suitable for diagnostic kit applications, as it retains full activity at up to 6 M GdmCl and 5% SDS (at 55 °C).[7]

Subtilisin E is a serine alkaline protease, and can be considered as an attractive alternative, as mesophilic subtilisins have also been reported to have considerable resistance towards GdmCl and SDS.[8] Besides, subtilisin E production is well established in *Bacillus subtilis*, while Tk-subtilisin was always overexpressed in *E. coli* as inclusion bodies requiring further solubilization and refolding.[9] In addition, successful protease re-engineering reports on improved activity and stability in organic solvents have been published for subtilisin E.[10] Finally, a subtilisin E crystal structure is available, which is an important prerequisite for generating hypotheses on GdmCl and SDS resistance of improved subtilisin E variants.[11]

Directed protease evolution, by iterative cycles of diversity generation and screening, has proved to be a reliable technique to improve protease properties such as substrate specificity, thermal resistance, and stability in organic solvents.[12] In addition, only two reports have been published on improving enzymes' resistance to detergent by directed evolution or semirational design. In the first report, several rounds of in vivo gene shuffling in yeast was applied to *T. lanuginose* lipase so as to improve its stability in the presence of detergent for washing applications. Several improved lipase variants were

[a] Z. Li, Prof. Dr. U. Schwaneberg
Lehrstuhl für Biotechnologie, RWTH Aachen University
Worringerweg 1, 52074 Aachen (Germany)
E-mail: u.schwaneberg@biotec.rwth-aachen.de

[b] Z. Li, Prof. Dr. D. Roccatano
School of Engineering and Science, Jacobs University Bremen
Campus Ring 1, 28759 Bremen (Germany)

[c] Prof. Dr. M. Lorenz
Molzym GmbH & Co. KG
Mary-Astell-Strasse 10, 28359 Bremen (Germany)

Supporting information for this article is available on the WWW under http://dx.doi.org/10.1002/cbic.201100714.

 © 2012 Wiley-VCH Verlag GmbH & Co. KGaA, Weinheim

obtained, and most of the lipid on clothing was removed after one wash cycle.[13] In the second report, Danielsen et al. selected nine amino acids in the hinge region of a lipase, lipolase, to overcome the inhibitory effects of detergent. Despite proving that the system yielded enriched populations, no improved variant could be isolated.[14]

Several theoretical studies, in particular those using molecular dynamics (MD) simulations, have been reported on urea and GdmCl effects on protein structures.[15] Although the molecular mechanisms still remains unclear and debated, these studies have given clues about the solvation mechanisms of urea and GdmCl. In the case of GdmCl, different MD simulations on peptides showed preferential solvation by guanidinium ions with aromatic groups over aliphatic groups (the solvation targets of denaturants such as urea).[16]

In this study, we report the first directed evolution strategy in which protease stability was improved in a chaotropic salt (GdmCl) or a detergent (SDS). Subtilisin E was engineered into a chaotolerent protease, and multiple screenings were used to maintain the proteolytic activity of subtilisin E against complex protein substrates. MD simulations provided the first insights into Gdm^+ interactions with subtilisin E.

Results

Scheme 1 shows the mutant library screening procedure (pre-screening in agar plates, and microtiter-plate-based screening) to identify subtilisin E variants with improved resistance, by detection of fluorescent from succinyl-L-Ala-L-Ala-L-Pro-L-Phe-4-methyl-coumaryl-7-amide (Suc-AAPF-AMC) while preserving activity towards complex substrates (skimmed milk activity detection, "skim-milk"). The following paragraphs describe the results of library generation, screening systems, and improved variant generation. Each microtiter plate was screened for activity towards complex substrates (skim-milk), and for absolute activity in the absence or presence of denaturants, GdmCl or SDS (with Suc-AAPF-AMC).

General remarks on screening systems and directed evolution strategies

Screening with 1% skim-milk agar plates was used to preselect active subtilisin E variants. Active variants were subjected to subsequent screening in 96-well microtiter plates (MTPs) in the absence and presence of GdmCl or SDS by using two substrates (Scheme 1). Coefficients of variations by 96-MTP-based Suc-AAPF-AMC screening were determined to be 10.9% (1 M GdmCl), 7.0% (0.5% SDS), and 6.5% (no denaturant), and the coefficient of variation in skim-milk detection was determined to be 16.8%. Coefficients of variation below 20% in MTP have been commonly accepted in directed evolution experiments.[17] To identify improved subtilisin E variants, the resistance ratio (to denaturant GdmCl or SDS) and activity ratio (with substrates Suc-AAPF-AMC or skim-milk) were calculated as follows [ratios (1) and (2)]:

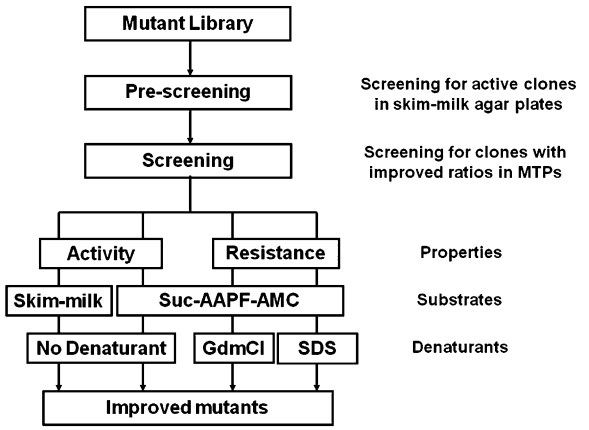

Scheme 1. Screening procedure employed in each round of directed evolution. Pre-screening with skim-milk agar plates for active variants is followed by two 96-well microtiter plate screening systems. These quantify subtilisin E variants for protease efficiency with complex protein substrates, and for GdmCl/SDS resistance.

$$\text{Resistance ratio (denaturant)} = (A(+)\text{denaturant}/A(-)\text{denaturant})_{\text{variant}}/(A(+)\text{denaturant}/A(-)\text{denaturant})_{\text{WT}} \quad (1)$$

$$\text{Activity ratio (substrate)} = A_{\text{variant}}/A_{\text{WT}} \quad (2)$$

In Ratio (1), the activity A in the presence of denaturants with Suc-AAPF-AMC as substrate is divided by that in the absence to eliminate expression mutants that only increase expression level rather than denaturant resistance. Ratio (1) quantifies improvement relative wild-type (WT). Ratio (2) gives a measure of the ability of subtilisin E variants to convert substrates. This is an important prerequisite, especially with complex proteins, for application in diagnostic kits. Both ratios were taken into account for selecting beneficial subtilisin E mutants in the three rounds of directed evolution.

Random mutagenesis and screening of libraries

Error-prone PCR (epPCR) libraries were generated by using various concentrations of $MnCl_2$ (0.05–0.50 mM) with unbalanced deoxyribonucleotide triphosphates (dNTP; dGTP ⩾ dATP = dCTP = dTTP). In three iterative rounds of directed evolution, two epPCR mutant libraries and one SeSaM (sequence saturation mutagenesis) library[18] were screened by sampling (~1300 clones per library). Conditions were selected after mutagenesis assistant program (MAP) analysis[19] to maximize charge substitutions. Substitutions with charged residues was regarded as beneficial on the assumption that charged residues on the surface improve interactions with cosolvents. A concentration of 0.1 mM $MnCl_2$ coupled with unbalanced dNTP (0.4 mM dGTP, 0.2 mM dATP, dCTP, and dTTP) resulted in about 50% active mutants, so was selected for the generation of both epPCR libraries. The SeSaM mutant library yielded about 33% active variants. Microtiter plate screening in the presence and absence of 1 M GdmCl or 0.5% SDS, and skim-milk activity screening were performed in parallel (Figure 1. Variants with

 © 2012 Wiley-VCH Verlag GmbH & Co. KGaA, Weinheim

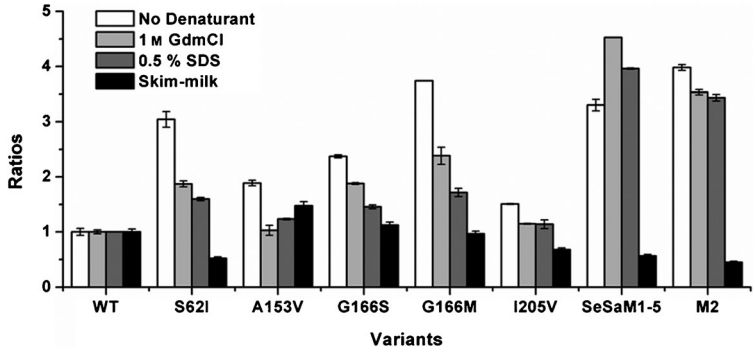

Figure 1. Activity and resistance ratios of subtilisin E variants in the presence or absence of denaturants. Ratios for subtilisin E variants were calculated according to Ratio (2) after enzyme assays in cell-free extracts by using an Agilent Protein 230 Kit with skim-milk or Suc-AAPF-AMC as substrate in the absence or presence of 1 M GdmCl or 0.5% SDS. Activity and resistance was measured in triplicate and are presented as U mg^{-1} with standard deviation.

a ratio(2) >0.3 (skim-milk assay) were further screened with Suc-AAPF-AMC for improved resistance, and variants with a ratio (1) >1.2 (first round), >1.5 (second round), and >2.5 (third round) were used for diversity generation in the subsequent round of directed evolution. Finally, eight mutants from the SeSaM library were rescreened and sequenced. The most beneficial variant, SeSaM1–5, showed a 4.53-fold increase in resistance to GdmCl (1 M; residual activity, 19%–87%) and a 3.96-fold increase with SDS (0.5%; residual activity 32%–127%; Figure 1 and Table S1 in the Supporting Information).

Site-directed and saturation mutagenesis

Sequencing results showed there were four mutations in SeSaM1–5 (M4): S62I (AGT→ATC), A153V (GCC→GTC), G166S (GGC→AGC), and I205V (ATC→GTC). The double-nucleotide mutation S62I (AGT→ATC) could only be obtained from the SeSaM library. Site saturation mutagenesis (SSM) studies were carried out by substitution at each position in WT subtilisin E to quantify individual contributions. Results showed that two positions (62 and 166) contributed mainly to the improved resistance towards GdmCl and SDS (Scheme 2). SSM at positions 153 and 205 did not generate improved resistance (Figure 1), while SSM at position 62 again yielded S62I as the most beneficial. SSM at position 166 yielded the "best" variant (G166M instead of G166S), which proved more resistant (Figure 1). Finally a double mutant (M2; S62I and G166M) was generated by site-directed mutagenesis. Comparison of the performance of M2 and SeSaM1–5 (M4) showed comparable activity with skim-milk. For GdmCl and SDS resistance, SeSaM1–5 performed slightly better than M2 under the screening conditions. This indicates a cooperative effect of the SeSaM1–5 substitutions with Suc-AAPF-AMC.

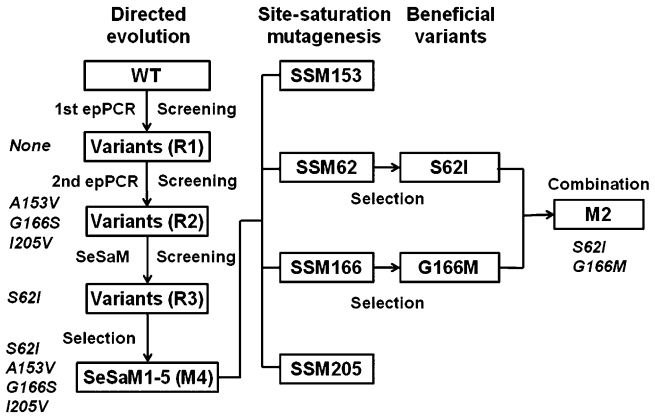

Scheme 2. Substitutions obtained in three rounds of directed evolution. Italicized substitutions show the rounds of directed evolution that obtained amino acid substitution is that finally yielded SeSaM1–5 (M4), the best mutant. Combination experiments were subsequently performed to quantify the contribution of each of four positions by site saturation mutagenesis of WT subtilisin E. Position S62 and G166 contributed mainly to GdmCl and SDS resistance and were combined to produce variant M2 (S62I, G166M).

Kinetic characterization of subtilisin E and variants

Figures 2 and S2 summarize the kinetic data (k_{cat}, K_m and k_{cat}/K_m) of purified WT subtilisin E and the obtained subtilisin E variants (S62I, G166M, M2, and M4).

In the absence of GdmCl or SDS, the k_{cat} values improved (WT: 50 s^{-1}, G166M: 141 s^{-1}, M2: 123 s^{-1}, S62I: 102 s^{-1}), although SeSaM1–5 had a lower k_{cat} value (42 s^{-1}). In the presence of 2 M GdmCl, specific activities decreased (WT: 15 s^{-1},

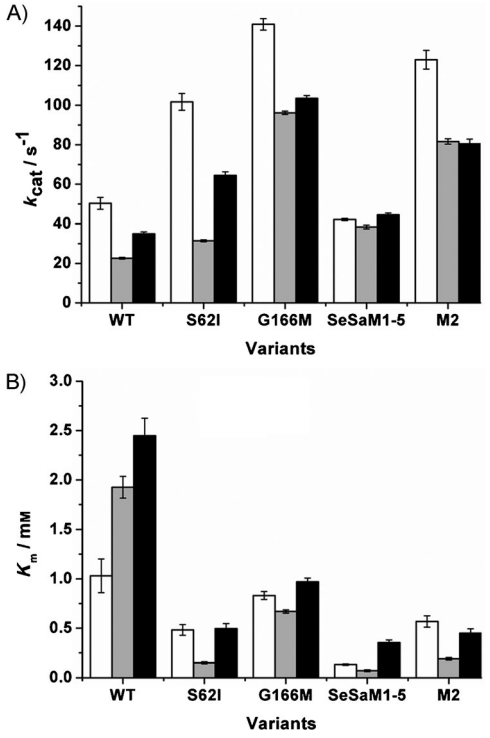

Figure 2. Kinetic constants of subtilisin E wild-type and variants in the absence and presence of denaturants with Suc-AAPF-pNA as substrate. □: no denaturant, ■: 1 M GdmCl, ■: 0.5% SDS. Values are mean (SD) of three separate determinations.

 © 2012 Wiley-VCH Verlag GmbH & Co. KGaA, Weinheim

SeSaM1–5: 34 s^{-1}), although those of M2 and G166M (62 and 70 s^{-1}, respectively) were higher than that of SeSaM1–5 (Figure S2). In the presence of SDS, a similar trend was observed (WT (35 s^{-1}) < SeSaM1–5 (45 s^{-1}) < S62I (65 s^{-1}) < M2 (81 s^{-1}) < G166M (104 s^{-1})).

Interestingly the K_m value for SeSaM1–5 (M4) was significantly reduced compared to WT when in GdmCl (up to 8-fold (no denaturant), 28-fold (1 M), and 46-fold (2 M)) and to SDS (sevenfold (0.5%); Figure 2 and Figure S2).

In the absence of GdmCl or SDS, the catalytic efficiency improved (G166M (threefold) < S62I (fourfold) ≈ M2 (fourfold) < SeSaM1–5 (sixfold)). It improved significantly in the presence of 2 M GdmCl (G166M (22-fold) < S62I (45-fold) < SeSaM1–5 (100-fold) < M2 (118-fold)), and in presence of 0.5% SDS (G166M (sevenfold) < SeSaM1–5 (ninefold) ≈ S62I (ninefold) < M2 (13-fold)).

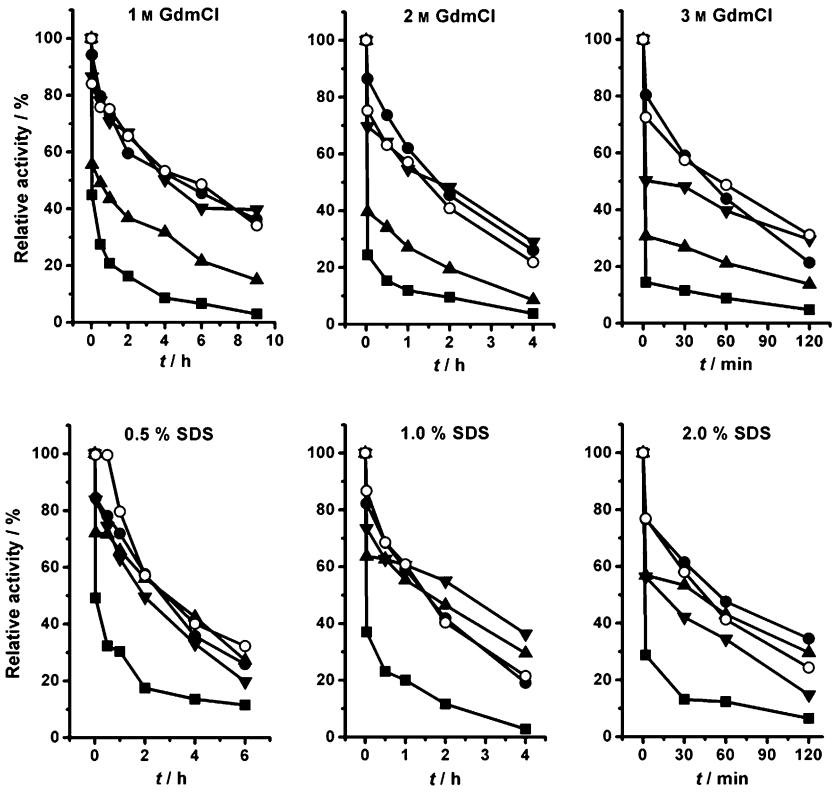

Figure 3. Stability of purified subtilisin E wild-type and its variants in the presence of GdmCl or SDS, by determining residual proteolytic activity (Suc-AAPF-pNA assay, 25 °C). Relative activities were measured in triplicate and averaged (< 10% standard deviation) and are shown relative to activity in the absence of denaturing reagents (100%). Protease concentration was 50 nM, protease protein content > 85%. ■: wild-type (WT), ▼: G166M, ▲: S62I, ●: SeSaM1–5 (M4), ○: M2.

Stability of subtilisin E variants in the presence of GdmCl and SDS

Figure 3 shows that all subtilisin E variants were more stable in the presence of all concentrations of denaturants compared to WT, which lost more than 50% of its activity when exposed to GdmCl or SDS (in > 2 min), thereby making a half life estimation challenging.

In 3 M GdmCl the half lives were < 2 min (WT), < 2 min (S62I), 5.7 min (G166M), 47.9 min (SeSaM1–5), and 55.7 min (M2); Similar results were obtained with 2 M and 1 M GdmCl. In particular, at 3 M GdmCl, M2 was significantly more stable than SeSaM1–5. A CD spectral analysis of purified SeSaM1–5 showed no detectable unfolding at the inhibitory concentration (1 M GdmCl, data not shown).

At 2% SDS, the half lives were < 2 min (WT), 39.9 min (S62I), 14.5 min (G166M), 54.8 min (SeSaM1–5), and 44.4 min (M2). At 1% SDS, these were < 2 min (WT), 1.6 h (S62I), 2.5 h (G166M), 1.5 h (SeSaM1–5), and 1.5 h (M2), and at 0.5% SDS, they were 2 min (WT), 2.9 h (S62I), 2.0 h (G166M), 2.7 h (SeSaM1–5) and 2.8 h (M2). In contrast to the case with GdmCl, the order of resistance of the four mutants depended highly on SDS concentration. In 2% SDS, SeSaM1–5 (M4) had the highest half life, whereas M2 was more resistant than SeSaM1–5 in 3 M GdmCl.

Molecular dynamics simulations

MD simulations (50 ns) of subtilisin E in water and 5 M GdmCl were performed. In Figure S3 A, the backbone root mean square deviations (RMSDs) are reported for the crystal structures in each simulation. RMSD curves reach an average plateau value of ~0.15 nm. Furthermore, the RMS deviations and fluctuations per residue (Figure S3 B and C) show that the protein residues undergo similar average conformation changes and have similar motilities in both water and GdmCl, other than for loop region 20–26. The apparent stability of the protein in the GdmCl simulation can be explained by considering the expected timescale of the unfolding process. In fact, in a recent in silico study, the unfolding of a lysozyme mutant (less stable than the wild-type) in 8 M urea required 1000 ns MD simulations at 310 K.[20] In light of recent experimental evidence of a more direct and faster mechanism of urea-induced (than GdmCl-induced) unfolding,[21] it is unlikely that a GdmCl-mediated unfolding event in our 50 ns simulations would be observed. Nevertheless, it is evident from experimental data on many enzymes that disturbance by GdmCl at the active sites occurs prior to conformational changes in the enzyme as a whole.[22] Gdm^+ binding to subtilisin E in close proximity to the active sites can occur in time scales shorter than those of denaturation. Therefore our MD simulations provide valid data for Gdm^+ binding to subtilisin E. The spatial density function

 © 2012 Wiley-VCH Verlag GmbH & Co. KGaA, Weinheim

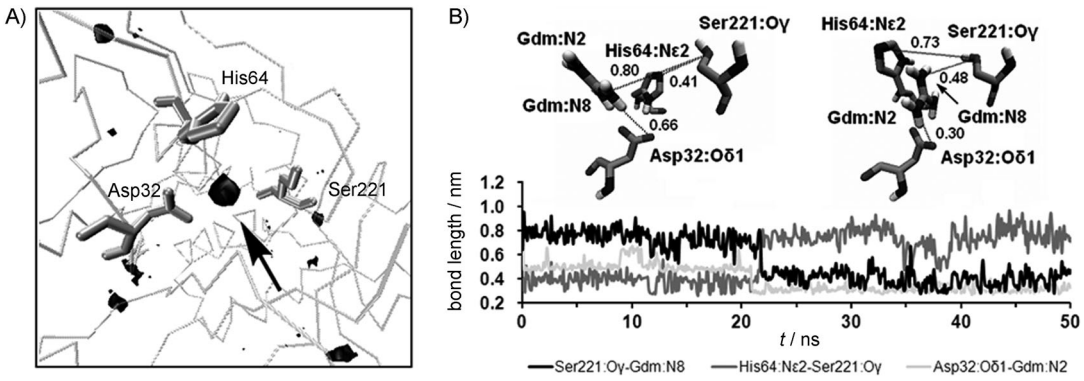

Figure 4. Analysis of Gdm^+ coordination in MD simulation of wild-type subtilisin E (5 M GdmCl). A) Active site region of wild-type subtilisin E with distribution of Gdm^+ ions during last 25 ns of simulation with the g_spatial program. Catalytic triad residues (Asp32, His64 and Ser221) are labeled. The Gdm^+ counters in the active site of subtilisin E are highlighted (arrow). B) Changes in the lengths of hydrogen bonds between Gdm^+ (N2 and N8) and Asp32 (Oδ1) and Ser221 (Oγ), and between His64 (Nε2) and Ser221 (Oγ) during the 50 ns simulation. Two snapshots of catalytic triad with one Gdm^+ ion (left, 10.8 ns; right, 37.6 ns) show a transition state after 21.8 ns that results in Gdm^+ bond-flip to Asp32 and Ser221 at the active site.

of Gdm^+ ions is shown in Figure 4; The "blobs" represent isosurfaces with high Gdm^+ density and are mainly localized at the active site around the catalytic triad. Analysis of the binding process during the simulation revealed the following sequence of events. First, a Gdm^+ ion diffuses into the active site (at 21.8 ns) and binds to the catalytic triad residue by facing the imidazole ring of His64 and forming two strong hydrogen bonds (to Ser221 and Asp32; Figure 4B). The presence of the Gdm^+ in the active side weakens the hydrogen bond between His64:Nε2 and Ser221:Oγ, which is essential for proteolytic activity. Two additional Gdm^+ ions diffused to the active site during the simulation (50 ns; Figure S4), by surrounding the active site residue in similar way as the first Gdm^+. Gdm^+ ions were also observed to accumulate in the substrate binding pocket, P1, near Gly166 (Figure S5). Gdm^+ ions might interact with Gly166 as well as simply blocking the substrate-specific pocket.

These results suggest that Gdm^+ ions are strongly bound to the active site residues thereby weakening H-bond networks (Figure 4B). This might cause very fast inactivation of subtilisin E, and provides a possible explanation for the increased tolerance of variant S62I, whose substitution is proximal to His64.

Discussion

Understanding the principles that control the activity and stability of proteases[23] in chaotropic salts and detergents is a poorly explored research area, despite its significance in applications (e.g., diagnostic kits). Only one rational design study (cutinase resistance) against a specific anionic detergent (dioctyl sulfosuccinate sodium salt, AOT) has been reported; the authors postulated that surface substitutions are the main contributors to detergent tolerance in cutinase.[24] No protein engineering study has hitherto been published that used directed protease evolution with the denaturants SDS and GdmCl. In our directed-evolution experiment, we aimed to gain insight into how subtilisin E could be engineered into a chaotolerant protease. Scheme 2 shows the substitutions and combinations found after three iterative rounds of directed evolution and subsequent site saturation. This identified Ser62 and Gly166 as key residues for stability in the presence of SDS and GdmCl.

The performances of WT subtilisin E, the best variants from three iterative rounds of directed evolution (SeSaM1–5), and the mutational studies (S62I, G166M and M2 (S62I and G166M)) are now compared.

SeSaM1–5 (M4) was obtained from random-mutagenesis experiments and contains four substitutions that are located in close proximity to active site residues (Figure 5). Site-directed mutagenesis revealed that, of the single substitutions, only S62I and G166S contribute to GdmCl and SDS resistance. Figure 3 shows that modification of Gly166 is the most beneficial for GdmCl and SDS resistance (M2 (G166M) and SeSaM1–5 (G166S)). Interestingly, in 2% SDS the quadruple mutant, SeSaM1–5, outperformed the G166M single substitution and

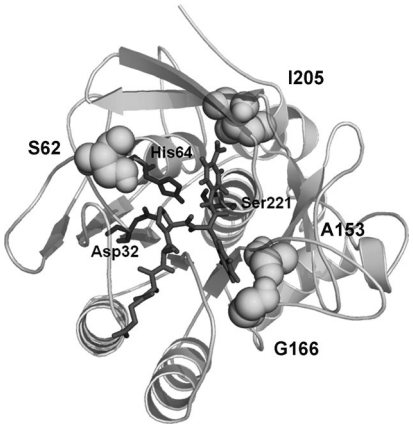

Figure 5. Subtilisin E wild-type structure with the colorimetric substrate Suc-Ala-Ala-Pro-Phe-pNA. Four amino acid substitutions (S62, A153, G166, I205; spheres) obtained by directed evolution are labeled, with the catalytic triad (black) and substrate (dark gray). The model was generated based on crystal structure complex of subtilisin E (PDB ID: 1SCJ). The pro-peptide sequence was replaced with Suc-Ala-Ala-Pro-Phe-pNA at the C terminus, followed by relaxation and energy minimization in vacuum using Gromacs 4.0 (see text).

 © 2012 Wiley-VCH Verlag GmbH & Co. KGaA, Weinheim

the double mutant, M2. This clearly indicates a cooperative effect between the four amino acids in SeSaM1–5 (M4), as no effect was found in the individual substitutions by site-saturation mutagenesis (Figures 1 and 2). In terms of catalytic performance, G166M is attractive for application in diagnostic kits as the activity towards the complex protein substrate (skim-milk) was not reduced relative to wild-type, while the resistance towards GdmCl was dramatically improved (Figure 3)—higher than that of SeSaM1–5. In addition, SDS tolerance was also significantly improved compared to WT (Figure 3), and the specific activity towards succinyl-L-Ala-L-Ala-L-Pro-L-Phe-4-nitroanilide (Suc-AAPF-pNA) was the highest among all mutants (Figure 2).

Mutations of Gly166 and Ser62 have been reported to influence substrate specificity.[25] Indeed, modification at Ser62 improved resistance towards GdmCl and SDS (Figure 3); however, the substitution reduced (~50%) activity towards the complex substrate, skimmed milk. SeSaM1–5 (with the S62I substitution) showed a comparable reduced activity towards skimmed milk, and was the best for resistance to 2% SDS.

The obtained substitutions were, in contrast to our expectations, not acidic amino acids on the surface of subtilisin E, although they are more prominent on the surface of halophilic enzymes.[26] The lack of substitutions to charged amino acids might indicate that charges on the surface of halophilic proteases contribute less to stability in the presence of the chaotropic salts. Interestingly the G166S substitution in SeSaM1–5 is also found in the hyperthermophilic subtilisin, Tk-subtilisin, at the corresponding position.[27]

Figure 5 shows the four mutations at the active site together with the substrate Suc-Ala-Ala-Pro-Pre-pNA. The model suggests that substitutions S62I or S62L might reduce the flexibility of His64 due to extension of side chains, or that it is displaced by S62F (Figures S4 and S6). Interestingly, during the simulation Gdm^+ ions were consistently observed around G166 (Figure S5). The increase in tolerance of the G166M and G166S variants could be a consequence of the presence of side chains that exclude Gdm^+ from the specificity pocket (see substitutions G166F or G166Y in Table S6).

MD simulations further suggested that Gdm^+ might interact directly with active site residues of WT subtilisin E (e.g., with His64; Figure 4), thereby leading to hydrogen bonding of Gdm^+ to Ser221 and Asp32. Therefore, GdmCl might inactivate subtilisin E by interfering with substrate binding. It has previously been proposed that Gdm^+ binding occurrs at the active site of subtilisin E prior to molecular conformational changes, as indicated by MD simulation.[22] Mutations that dramatically decreased K_m (Figure 2) often increased affinity to the peptide substrate (Suc-AAPF-pNA), while most likely reduce the flexibility of the active site. Therefore, tight substrate binding assists in excluding GdmCl from the active site, threby resulting in increased GdmCl resistance. However, the activity with complex substrates, such as skimmed milk, was often reduced (Figure 1) due to decreased flexibility of the active site.[22] Similar stabilization against denaturation in dilute GdmCl was observed in muscle lactate dehydrogenase H_4 (glutaraldehyde crosslinking or in concentrated ammonium sulfate solution); reduced flexibility led to a decrease in activity.[28] Furthermore, simulations suggested that Gdm^+ binding happens in two stages: interaction with His64, then a resulting displacement of His64 which results in tighter binding of Gdm^+ (Figure 4). All four positions identified in subtilisin E (Figure 5) are in contact with or in close proximity to active site residues. In particular, substitution S62I might prevent His64 displacement and Gdm^+ disturbance.

Interactions between proteins and denaturants, especially urea and GdmCl, have been studied for many years. An early hypothesis postulated that urea and GdmCl perturb hydrogen bonding in water, and thus indirectly destabilize folded protein. More recently, new hypotheses have been developed and debated,[15] for instance, that denaturants affect a protein's hydration shell rather than the bulk solvent. In a simulation study on lysozyme, urea displaced water from the hydration shell and penetrated into the hydrophobic core, thereby destabilizing the native fold.[20] For GdmCl, a different and surfactant-like denaturation mechanism has been proposed in which Gdm^+ sticks to hydrophobic surface residues (preferring aromatic groups over aliphatic).[16b,29] As mentioned above, our MD simulations were too short to provide insights into GdmCl-mediated denaturation mechanisms. However, a tendency to accumulate around aromatic residue was also observed in our simulations.

Notably, despite the harsh screening conditions (the half life of WT subtilisin E in 1 M GdmCl or 0.5% SDS is <2 min), significantly improved subtilisin muteins were isolated (half lives up to 5.4 h in 1 M GdmCl and 2.8 h in 0.5% SDS).

Simultaneous improvement in resistance to GdmCl and SDS was unexpected, as denaturation mechanisms and interactions with the molecular surface differ.[30] An additional challenge with SDS is that it behaves differently before and after it reaches critical micelle concentration (CMC; 8.1 mM).[31] In the screening setup, concentrations were above the CMC (0.5% SDS, 17.3 mM) in order to obtain subtilisin E improvements under conditions which mimic those of the intended applications.

It should further be noted that it is very unusual in directed evolution experiments that four substitutions are located around the active site, especially as only a few thousand variants were sampled.[32] It might therefore be informative to test semirational investigation on the role of amino acid positions in close proximity to the active site by site-directed mutagenesis (SDM) or multi-site saturation,[33] in order to stabilize subtilisin E by preventing access of Gdm^+ ions to the active site.

Conclusion

In summary, three iterative rounds of directed evolution and subsequent site-saturation mutagenesis studies revealed that substitutions at positions 62 and 166 improved subtilisin E resistance to GdmCl and SDS denaturation. For the first time subtilisin E was engineered into a chaotolerent protease (half life 55.7 min for M2 in 3 M GdmCl, <2 min for WT). MD simulation led to the hypothesis that Gdm^+ ions might directly interact with active-site residues, although this should be studied

 © 2012 Wiley-VCH Verlag GmbH & Co. KGaA, Weinheim

computationally in more detail. The unusual finding that all four substitutions surround active-site residues in subtilisin E demonstrates the benefit of mutating amino acids close to active-site residues to stabilize subtilisin E against GdmCl. This approach might be of general interest for serine protease stabilization.

Experimental Section

All chemicals were of analytical reagent grade or higher quality and were purchased from Merck, Fluka, Sigma–Aldrich, and Applichem (Darmstadt, Germany), except the resins for purification (TOSOH, Stuttgart, Germany). All enzymes were purchased from New England Biolabs, Fermentas, and Sigma–Aldrich, unless otherwise stated. The fluorescent substrate Suc-AAPF-AMC was purchased from Bachem AG (Bubendorf, Switzerland), and Suc-AAPF-pNA was purchased from Sigma–Aldrich.

A thermal cycler (Mastercycler gradient; Eppendorf) and thin-walled PCR tubes (0.2 mL Multi-ultra tubes; Carl Roth, Germany) were used in all PCR reactions. The PCR volume was always 50 μL; larger volumes were prepared as multiple 50 μL PCRs. The amount of DNA in cloning experiments was quantified by using a NanoDrop photometer (Thermo Scientific, Wilmington, USA).

Cloning and expression of subtilisin E in *B. subtilis*: The subtilisin E gene (*aprE*) was ordered as synthetic gene (Geneart, Regensburg, Germany), cloned into the commercial shuttle vector pHY300PLK (Takara Bio Inc, Japan) to yield pHY-*aprE*, and transformed after replication (REPLI-g Mini Kit; Qiagen, Hilden, Germany) into *B. subtilis* WB600, the six-protease-deficient strain that was used as host strain for all directed evolution and focused mutagenesis studies. Subtilisin E was expressed in LB medium containing 15 $\mu g\,mL^{-1}$ tetracycline, and achieved maximum active, soluble protease production after 36 h of growth on a shaker (37 °C, 250 rpm).

Construction of error-prone PCR libraries: The NdeI–BamHI DNA fragment of pHY-*aprE* encodes the mature subtilisin E and was selected as the template for random mutagenesis. The phosphorothioate-based ligase-independent gene cloning (PLICing) method was applied for all cloning procedures.[34] Two oligonucleotides, 5′-A*T*C*C*G*A* G*C*G*T*T*G* CATATG TGGAAG AAGATC ATATTG CACATG AA-3′ (gF), 5′-C*T*G*C*A*G* G*T*C*G*A*C* GGATCC TTATTG TGCAGC TGCTTG TACGTT GAT-3′ (gR, * indicates bases attached with phosphorothioate; restriction sites are underlined) were used as forward and reverse primers to amplify the mature subtilisin E. The epPCR libraries were generated by using template (pHY-*aprE*, 50 ng), dNTP mix (0.2 mM), dGTP (0.2 mM), $MnCl_2$ (0.05–0.5 mM), Taq DNA polymerase (5 U), forward and reverse primers (20 pmol) under the following PCR conditions: 94 °C 2 min; 94 °C 30 s, 60 °C 1 min, 72 °C 1 min (29 cycles); 72 °C 5 min.

The vector fragment pHY-*aprE*$^-$ was amplified by using template (pHY-*aprE*, 50 ng), dNTP mix (0.2 mM), betaine (1 M), Taq/Pfu DNA polymerase (4.5 U/0.072 U) and primers 5′-C*A*A*C*G*C* T*C*G*G*A*T* CTTTTT TCAATT CTTTTA CAGCT-3′ (pF) and 5′-G*T*C*G*A*C* C*T*G*C*A*G* ATCTCT AGAAGC TTGGGC AAAGC-3′ (pR, * indicates bases attached by phosphorothioate) under the following PCR conditions: 94 °C 2 min; 94 °C 30 s, 60 °C 30 s, 68 °C 9 min (35 cycles); 68 °C 10 min. The resulting PCR products of pHY-*aprE*$^-$ were purified by using a Qiagen PCR purification kit. The purified pHY-*aprE*$^-$ and epPCR products were digested by DpnI (40 U; New England Biolabs) at 37 °C overnight, followed by further DNA purification (Qiagen quick PCR purification kit). Both fragments (0.1 pmol pHY-*aprE*$^-$ and 0.3 pmol epPCR products) were further digested by iodine mixture at 70 °C for 10 min, and then mixed at room temperature for 30 min for ligation. The ligation mixture was transformed into *E. coli* DH5α and plated on LB-Amp agar plates. Thousands of *E. coli* DH5α variants were harvested by resuspending in double-distilled water and subsequent plasmid isolation (Qiagen Spin Miniprep Kit). The resulting plasmid pool was then transformed into *B. subtilis* WB600 as described above for expression and screening. Ten randomly picked and sequenced variants of epPCR library 1 confirmed the expected mutational bias (within statistical error).

Construction of SeSaM[18] library: The SeSaM library was generated, with the improved variants selected after two rounds of epPCR library screening as template. The generation of the SeSaM library was carried out according to the handbook (SeSaM Tv Classic version 0.16; SeSaM-Biotech GmbH, Bremen, Germany). The PLICing method was used for cloning. PCR was carried out by using a SeSaM library as template (50 ng), dNTP mix (0.2 mM), Pfu DNA polymerase (2.5 U), with forward and reverse primers (gF and gR, 20 pmol) under PCR conditions: 98 °C 30 s; 98 °C 5 s, 60 °C 15 s,72 °C 15 s (15 cycles); 72 °C 3 min. Further cloning was carried out according to the procedure described above.

Site-directed and saturation mutagenesis: SD) and saturation mutagenesis of WT subtilisin E was employed to elucidate the role of each substitution found in SeSaM1–5 (M4). SSM was performed at positions 62, 153, 166 and 205. SDM was employed to generate single mutants of subtilisin E (S62I, A153V, G166S and I205V) and one double mutant, M2 (S62I/G166M). The latter was generated after screening of all SSM libraries. In all focused mutagenesis experiments, a modified QuikChange (Stratagene/Agilent Technologies) method was used.[35]

Cultivation and expression in 96-well plates: Active colonies which showed halos when grown on LB-tet agar plates with skimmed milk (1%) as substrate were transferred by toothpicks into 96-well microtiter plates (V-bottomed, polystyrene plates; Greiner Bio-One GmbH, Frickenhausen, Germany) containing LB medium (150 μL) supplemented with tetracycline (15 $\mu g\,mL^{-1}$ per well). After 16 h of cultivation in a Multitron II microtiter plate shaker (Infors GmbH, Einsbach, Germany; 37 °C, 900 rpm, 70% humidity), each 96-well microtiter plate was replicated (replicator tool; EnzyScreen BV, Leiden, Netherlands) into a 96-well microtiter plate containing the same medium, and cultivated in LB-tet medium in a Multitron II (24 h, 37 °C, 900 rpm, 70% humidity; Infors). Subtilisin E and variants were constitutively expressed and the cell cultures from microtiter plates were centrifuged (3220 *g*, 4 °C, 20 min). The supernatants were directly used for screening.

Screening assays for activity and GdmCl/SDS resistance

Fluorimetric microtiter plate assay: The assay was carried out in 96-well microtiter plates (black, flat bottomed, polystyrene plates; Greiner Bio-One) with Suc-AAPF-AMC in Tris-HCl buffer (0.1 M, pH 8.5, 37 °C) in the presence or absence of GdmCl (1 M) or SDS (0.5%). The cell-free supernatants (10 μL) of the variants were supplemented with Tris-HCl buffer (40 μL, 0.1 M, pH 8.5), GdmCl (40 μL, 2.5 M in Tris•HCl (0.1 M, pH 8.5)) or SDS (40 μL, 1.25% in Tris•HCl (0.1 M, pH 8.5)), incubated (25 °C, 30 min), and activities were determined by supplementing with substrate solution (50 μL, Suc-AAPF-AMC (200 μM) in Tris•HCl (0.1 M pH 8.5)). The final reaction volume was 100 μL. Calcium was not supplemented into the SDS reaction assays despite its stabilizing function,[36] as it causes precipitation. The activity in the presence or absence of denaturants was mea-

 © 2012 Wiley-VCH Verlag GmbH & Co. KGaA, Weinheim

sured at 37 °C by monitoring the increase in fluorescence intensity within 20 min by using a Tecan SAFIRE ($\lambda_{ex}=350$ nm, $\lambda_{em}=450$ nm; Tecan Austria GmbH, Salzburg, Austria). One unit of enzymatic activity was defined as the amount of enzyme that produces 1 pmol of AMC per min. Specific activity is protease activity per milligram of protein.

Skim-milk microtiter plate assay: The assay was carried out in 96-well microtiter plates (flat-bottomed, polystyrene plates; Greiner Bio-One). The screening procedure was performed by using supernatants of subtilisin E variants (10 μL) in Tris·HCl buffer (90 μL, 0.1 M, pH 8.5) at 37 °C, and activities were determined by supplementing with the substrate solution (100 μL, 2.0% skimmed milk in Tris·HCl (0.1 M pH 8.5)). The final reaction volume was 200 μL. The activity was measured at 37 °C by monitoring the increase of absorbance at 580 nm within 15 min with a Tecan Sunrise.

Purification of subtilisin E wild-type and its variants: A 1 L shaking flask containing LB medium (150 mL) supplemented with tetracycline (15 μg mL^{-1}) was inoculated with a 1:150 dilution of an overnight culture (*B. subtilis* WB600 harboring pHY-*aprE*) grown in the same medium. After 36 h of expression, *B. subtilis* WB600 cells were harvested by centrifugation (3220 *g*, 4 °C, 30 min; Eppendorf 5810R), and the culture supernatant was purified by filtration (0.2 μm Minisart sterile syringe filter; Sartorius, Goettingen, Germany). The filtered solution was subsequently concentrated through a 5 kDa cut-off membrane (Millipore, Billerica, MA, USA) by using a stirred Amicon ultrafitration cell (Millipore) and transferred into Tris·HCl buffer (20 mL, 0.1 M, pH 7.5). Concentrated solutions of WT subtilisin E and variants S62I, G166M, M2 (S62I/G166M), and SeSaM1–5 (M4) were subsequently purified by ion exchange column chromatography: 1) Subtilisin E variants were loaded onto a Super-Q anion-exchange column (25 mL), and equilibrated with the same buffer. Subtilisin E was eluted by a linear gradient of NaCl (0 to 1.0 M) in the same buffer (2 mL min^{-1}, five column volumes in total). 2) The obtained protein solution was loaded onto a SP650c cation-exchange column (25 mL) that had been equilibrated with the same buffer. Subtilisin E eluted in the flow-through while other proteins remained bound. The SP650c cation-exchange column was regenerated by NaCl gradient elution (0 to 2.0 M, five column volumes in total) in the same buffer (3 mL min^{-1}). Purified subtilisin E variants were subsequently concentrated in an Amicon ultra centrifugal filter device (Millipore) with a 10 kDa cut-off membrane.

Normalization of protein concentration: Protein concentrations for screening were determined by using an Agilent 2100 Bioanalyzer (Agilent Protein 230 Kit; Agilent Technologies, Böblingen, Germany) and a BCA protein assay kit (#23225; Pierce Biotechnology, Rockford, IL) according to the manufacturer's instructions. BSA (200 μg mL^{-1}) was used as internal standard.

Enzyme kinetics: Measurements were carried out in 96-well microtiter plates (flat-bottomed, polystyrene plates; Greiner Bio-One) with purified protease solution (50 nM) in the presence of GdmCl (1 M or 2 M) or SDS (0.5%) in Tris-HCl buffer (0.1 M, pH 8.5), or in the absence of denaturant, with Suc-AAPF-pNA (0.05–10.0 mM). The amount of *p*-nitroaniline (pNA) released from Suc-AAPF-pNA was determined by absorbance (410 nm). One unit of protease activity was defined as the amount of protease that produced 1 μmol of *p*-nitroaniline per min. Specific activity is protease activity per milligram of protein. For kinetic analysis, k_{cat} and K_m values were determined from initial velocity data plotted as a function of substrate concentration with a linear correlation coefficient of >0.99.

Enzyme stability in the presence of GdmCl or SDS: Purified WT or variant subtilisin E (50 nM) was incubated (25 °C) in the presence of a given concentrations of GdmCl or SDS. At different time points (0, 0.5, 1, 2, 4, 6 and 9 h), the activity was determined by using Suc-AAPF-pNA as described above. Relative activities were recorded as percentages of initial activities in the presence and absence of denaturant. Activity in the absence of a denaturant was 100%.

Molecular modeling: The crystal structure of the pro-subtilisin E complex is available at 0.2 nm (PDB ID: 1SCJ).[11] In order to generate the structure of the subtilisin E–Suc-AAPF-pNA complex, the pro-peptide domain of the crystal structure was removed and discarded, except for the four amino acids (Ala-His-Glu-Tyr) at the C terminus that were used to bind with active site residues in an enzyme–substrate complex.[11] The four-amino-acid chain was then mutated computationally to the sequence Ala-Ala-Pro-Phe (AAPF) and functional groups, N-succinyl and *p*-nitroanilide were attached to the termini to form the substrate Suc-AAPF-pNA. The favorable rotamer was selected in all cases. Finally, the active site Cys221 (mutated in PDB ID: 1SCJ) was replaced with the catalytic serine. All amino acid exchanges were performed using the *mutate* tool of the program Swiss PDB Viewer[37] by selecting in all cases the favorable side chain rotamer. Two calcium ions (Ca1, Ca2) that were present in the crystal structure were retained for modeling. The final structures of the protein–substrate complex was subsequently energy minimized in vacuum using the Groms96 force field.[38]

Molecular dynamics simulation

The starting structure of subtilisin E for MD simulation was prepared as described in the molecular modeling section. In this case, the pro-peptide domain in the crystal structure was completely removed, as it is cleaved in the maturation process. GROMOS96 43a1 force field parameters were used for simulations.[38] Water was modeled using the Simple Point Charge model.[39] The GdmCl model was taken from C. Camilloni et al.[40] The MD simulations of subtilisin E were carried out in water and GdmCl (5 M) The simulation boxes were built by centering the subtilisin E molecule in a cube (8×8×8 nm). Subtilisin E was solvated by stacking an equilibrated box of 216 water molecules to completely fill the simulation box. All solvent molecules with any atom within 0.15 nm of solute atom were removed. The total charge of the box (+2) was neutralized by replacing two water molecules at the most positive electrostatic potential with two Cl^- ions. The GdmCl solution (5 M) was generated by placing 1139 Gdm^+ molecules and 1141 chloride ions in the cubic box with subtilisin E and adding water molecules to fill the remaining space.

Simulation protocol: Systems described in the previous paragraph were energy minimized by using the steepest descent method ($\geq$ 500 steps) to remove clashes caused by solvent molecules. Subtilisin E was studied at 298 K. All simulations were performed by keeping the temperature at the reference values by weak coupling (coupling constant $\tau=0.1$ ps) with an external bath.[41] The pressure of the system was kept constant (1 bar) by using the Berendsen barostat equation ($\tau_p=0.5$ ps). The LINCS algorithm was used to constrain all bond lengths.[42] For the water molecules, the SETTLE algorithm was used.[43] Dielectric permittivity was $\varepsilon_r=1$, and a time step of 2 fs was used. The nonbonded interactions (electrostatic and Leonard–Jones) were calculated using the Particle Mesh Ewalds (PME) method.[44] For calculation of long-range interactions, a grid spacing of 0.12 nm combined with a fourth-order B-spline interpolation was used, to compute the potential and forces between grid points. A nonbonded pair-list cut-off of 0.9 nm

 © 2012 Wiley-VCH Verlag GmbH & Co. KGaA, Weinheim

was used and the pair-list was updated every five time steps. The MD simulations were started by assigning all atoms with initial velocities obtained from a Maxwellian distribution at the given temperature. The box density was equilibrated (100 ps) by using position restraints on the protein heavy atoms. After the equilibration, the position restraints on the protein were removed and the system was gradually heated from 50 K to the simulation temperature over 50 ps and then equilibrated for 5 ns. The ensuing runs were 45 ns.

Analysis of trajectory: The protein structure along the two trajectories was monitored by standard analysis tools to assess deviations from the crystallographic structure and mobility. The distribution of the guanidinium ions around subtilisin E was analyzed using the spatial density distribution functions (SDF). The calculation of SDF was carried out on the last 25 ns of the simulations using the g_ spatial program of the Gromacs package (4.0). The resulting spatial distribution function (SDF) was visualized using the program VMD.[45]

Acknowledgements

We thank the Federal Ministry of Education and Research (BMBF, Biokatalyse2021 Project 0315291B) and the company Molzym (especially Prof. Dr. Michael Lorenz) for financial support.

Keywords: chaotolerant · directed evolution · guanidinium chloride · protein models · SDS · subtilisin E

[1] R. Gupta, Q. Beg, P. Lorenz, *Appl. Microbiol. Biotechnol.* **2002**, *59*, 15 – 32.
[2] a) H. C. Birnboim, J. Doly, *Nucleic Acids Res.* **1979**, *7*, 1513 – 1523; b) R. Boom, C. J. Sol, M. M. Salimans, C. L. Jansen, P. M. Wertheim-van Dillen, J. van der Noordaa, *J. Clin. Microbiol.* **1990**, *28*, 495 – 503.
[3] J. P. Williams, J. E. Hallsworth, *Environ. Microbiol.* **2009**, *11*, 3292 – 3308.
[4] R. E. De Castro, J. A. Maupin-Furlow, M. I. Giménez, M. K. Herrera Seitz, J. J. Sánchez, *FEMS Microbiol. Rev.* **2006**, *30*, 17 – 35.
[5] a) C. Sánchez-Porro, E. Mellado, C. Bertoldo, G. Antranikian, A. Ventosa, *Extremophiles* **2003**, *7*, 221 – 228; b) H. R. Karbalaei-Heidari, A. A. Ziaee, M. A. Amoozegar, *Extremophiles* **2007**, *11*, 237 – 243.
[6] K. Hecht, R. Jaenicke, *Biochemistry* **1989**, *28*, 4979 – 4985.
[7] T. Foophow, S. Tanaka, Y. Koga, K. Takano, S. Kanaya, *Protein Eng. Des. Sel.* **2010**, *23*, 347 – 355.
[8] a) M. Ottesen, I. Svendsen in *Methods in Enzymology, Vol. 19* (Eds.: G. E. Perlmann, L. Lorand), Academic Press, New York, **1970**, pp. 199 – 215; b) L. Owers Narhi, M. Zukowski, T. Arakawa, *Arch. Biochem. Biophys.* **1988**, *261*, 161 – 169.
[9] Y. Kannan, Y. Koga, Y. Inoue, M. Haruki, M. Takagi, T. Imanaka, M. Morikawa, S. Kanaya, *Appl. Environ. Microbiol.* **2001**, *67*, 2445 – 2452.
[10] L. You, F. H. Arnold, *Protein Eng.* **1996**, *9*, 77 – 83.
[11] S. C. Jain, U. Shinde, Y. Li, M. Inouye, H. M. Berman, *J. Mol. Biol.* **1998**, *284*, 137 – 144.
[12] P. N. Bryan, *Biochim. Biophys. Acta Protein Struct. Mol. Enzymol.* **2000**, *1543*, 203 – 222.
[13] J. S. Okkels in *Enzyme Functionality: Design, Engineering and Screening* (Ed.: A. Svendsen), Marcel Dekker, New York, **2003**, 378 – 389.
[14] S. Danielsen, M. Eklund, H. J. Deussen, T. Gräslund, P. A. Nygren, T. V. Borchert, *Gene* **2001**, *272*, 267 – 274.
[15] J. L. England, G. Haran, *Annu. Rev. Phys. Chem.* **2011**, *62*, 257 – 277.
[16] a) P. E. Mason, J. W. Brady, G. W. Neilson, C. E. Dempsey, *Biophys. J.* **2007**, *93*, L04 – 06; b) P. E. Mason, C. E. Dempsey, G. W. Neilson, S. R. Kline, J. W. Brady, *J. Am. Chem. Soc.* **2009**, *131*, 16689 – 16696.
[17] K. L. Tee, U. Schwaneberg, *Comb. Chem. High Throughput Screening* **2007**, *10*, 197 – 217.
[18] T. S. Wong, K. L. Tee, B. Hauer, U. Schwaneberg, *Nucleic Acids Res.* **2004**, *32*, e26.
[19] T. S. Wong, D. Roccatano, M. Zacharias, U. Schwaneberg, *J. Mol. Biol.* **2006**, *355*, 858 – 871.
[20] L. Hua, R. Zhou, D. Thirumalai, B. J. Berne, *Proc. Natl. Acad. Sci. USA* **2008**, *105*, 16928 – 16933.
[21] W. K. Lim, J. Rösgen, S. W. Englander, *Proc. Natl. Acad. Sci. USA* **2009**, *106*, 2595 – 2600.
[22] a) C. L. Tsou, *Science* **1993**, *262*, 380 – 381; b) C. L. Tsou, *Biochim. Biophys. Acta Protein Struct. Mol. Enzymol.* **1995**, *1253*, 151 – 162.
[23] C. von der Osten, S. Branner, S. Hastrup, L. Hedegaard, M. D. Rasmussen, H. Bisgård-Frantzen, S. Carlsen, J. M. Mikkelsen, *J. Biotechnol.* **1993**, *28*, 55 – 68.
[24] V. Brissos, T. Eggert, J. M. Cabral, K. E. Jaeger, *Protein Eng. Des. Sel.* **2008**, *21*, 387 – 393.
[25] M. D. Ballinger, J. Tom, J. A. Wells, *Biochemistry* **1995**, *34*, 13312 – 13319.
[26] a) J. K. Rao, P. Argos, *Biochemistry* **1981**, *20*, 6536 – 6543; b) M. Mevarech, F. Frolow, L. M. Gloss, *Biophys. Chem.* **2000**, *86*, 155 – 164; c) B. Bieger, L. O. Essen, D. Oesterhelt, *Structure* **2003**, *11*, 375 – 385.
[27] S. Tanaka, H. Matsumura, Y. Koga, K. Takano, S. Kanaya, *J. Mol. Biol.* **2007**, *372*, 1055 – 1069.
[28] Y. Z. Ma, C. L. Tsou, *Biochem. J.* **1991**, *277*, 207 – 211.
[29] J. L. England, V. S. Pande, G. Haran, *J. Am. Chem. Soc.* **2008**, *130*, 11854 – 11855.
[30] X.-Q. Wu, H. Xu, H. Yue, K.-Q. Liu, X.-Y. Wang, *Protein J.* **2009**, *28*, 448 – 456.
[31] A. K. Bhuyan, *Biopolymers* **2010**, *93*, 186 – 199.
[32] a) A. V. Shivange, J. Marienhagen, H. Mundhada, A. Schenk, U. Schwaneberg, *Curr. Opin. Chem. Biol.* **2009**, *13*, 19 – 25; b) H. Jochens, M. Hesseler, K. Stiba, S. K. Padhi, R. J. Kazlauskas, U. T. Bornscheuer, *ChemBioChem* **2011**, *12*, 1508 – 1517.
[33] A. Dennig, A. V. Shivange, J. Marienhagen, U. Schwaneberg, *PLoS ONE* **2011**, *6*, e26222.
[34] M. Blanusa, A. Schenk, H. Sadeghi, J. Marienhagen, U. Schwaneberg, *Anal. Biochem.* **2010**, *406*, 141 – 146.
[35] L. Zheng, U. Baumann, J. L. Reymond, *Nucleic Acids Res.* **2004**, *32*, e115.
[36] P. A. Alexander, B. Ruan, P. N. Bryan, *Biochemistry* **2001**, *40*, 10634 – 10639.
[37] N. Guex, M. C. Peitsch, *Electrophoresis* **1997**, *18*, 2714 – 2723.
[38] W. R. P. Scott, P. H. Hünenberger, I. G. Tironi, A. E. Mark, S. R. Billeter, J. Fennen, A. E. Torda, T. Huber, P. Krüger, W. F. van Gunsteren, *J. Phys. Chem. A* **1999**, *103*, 3596 – 3607.
[39] H. J. C. Berendsen, J. P. M. Postma, W. F. van Gunsteren, J. Hermans in *Intermolecular Forces* (Ed.: B. Pullman), Reidel, Dordrecht, **1981**, pp. 331 – 342.
[40] C. Camilloni, A. G. Rocco, I. Eberini, E. Gianazza, R. A. Broglia, G. Tiana, *Biophys. J.* **2008**, *94*, 4654 – 4661.
[41] H. J. C. Berendsen, J. P. M. Postma, W. F. Vangunsteren, A. Dinola, J. R. Haak, *J. Chem. Phys.* **1984**, *81*, 3684 – 3690.
[42] B. Hess, H. Bekker, H. J. C. Berendsen, J. G. E. M. Fraaije, *J. Comput. Chem.* **1997**, *18*, 1463 – 1472.
[43] S. Miyamoto, P. A. Kollman, *J. Comput. Chem.* **1992**, *13*, 952 – 962.
[44] U. Essmann, L. Perera, M. L. Berkowitz, T. Darden, H. Lee, L. G. Pedersen, *J. Chem. Phys.* **1995**, *103*, 8577 – 8593.
[45] W. Humphrey, A. Dalke, K. Schulten, *J. Mol. Graph.* **1996**, *14*, 33 – 38, 27 – 38.

Received: November 13, 2011
Published online on March 8, 2012

 © 2012 Wiley-VCH Verlag GmbH & Co. KGaA, Weinheim